Quantitative Susceptibility Mapping of Brain Iron Deposition in Patients with Recurrent Depression

Xinxiu Duan
Lianyungang first people's Hospital
Yuhang Xie
Affiliated hospital of jiangsu university
Xiufang Zhu
Lianyungang first people's Hospital
Lei Chen
Lianyungang first people's Hospital
Feng Li
Affiliated hospital of jiangsu university
Guoquan Feng
Affiliated hospital of jiangsu university
Lei Li (lileijs6969@126.com)
Lianyungang first people's Hospital

Research Article

Keywords: Iron, Biomarkers, Depression, Brain, Magnetic resonance imaging

Posted Date: October 25th, 2021

DOI: https://doi.org/10.21203/rs.3.rs-966339/v1

Abstract

Background

Recurrence is the most significant feature of depression and the relationship between iron and depression is still lack of direct evidence in vivo.

Purpose

To explore the relationships between the brain iron and the multiple recurrent depression using quantitative susceptibility mapping (QSM).

Methods

Twenty-one patients with depression (before and after treatment) and twenty control subjects were included. Gradient-recalled echo (GRE), T1 and T2 images were acquired using a 3.0T MRI system. After QSM were reconstructed and standardized, a whole-brain and the regions of interest (ROIs) were respectively analyzed using the permutation test and voxel-wise methods. In addition, regional QSM analysis and Pearson correlation test on the susceptibility of ROIs with depression-related conditions were performed.

Results

Significant increases in susceptibility were found in multiple recurrent depression patients, which involved several brain regions. Interestingly, no susceptibility changes after treatment compared to pre-treatment (all $P>0.05$) and no significant correlation between susceptibility and Hamilton Depression Rating Scale (HRDS) were found. Besides, it was close to significance that those with a higher relapse frequency or a longer mean duration of single episode had a higher susceptibility in the putamen, thalamus, and hippocampus. Further studies showed susceptibility across the putamen ($\rho^2 = 0.27$, $P<0.001$), thalamus ($\rho^2 = 0.21$, $P<0.001$), and hippocampus ($\rho^2 = 0.19$, $P<0.001$) were strongly correlated with total course of disease onset.

Conclusions

Brain iron deposition is related to the total course of disease onset, but not the severity of depression, which suggest that brain iron deposition may be a sign of brain damage in multiple recurrent depression.

Introduction

Depression is a complicated disease involving multiple biological processes and pathways[1–3], and its pathophysiology is still unclear.

Iron, an essential microelement in the body, plays important roles in physiological functions and the development of human brain, including oxygen transport, DNA synthesis and repair, electron transport, and neurotransmitter metabolism[4, 5]. Decrease of iron not only result in the accumulation of monoamine oxidase that significantly reducing catechol transmitters, but also preventing the degradation of serotonin and decreasing the density and activity of dopamine[6]. On the other hand, excessive iron deposition can prevent dopamine synthesis by inducing toxic free radicals, which is involved in emotional and cognitive processing[7, 8]. Although these reports have suggested the abnormal iron might influence the metabolism of depression related neurotransmitters from the side, the relationship between iron and depression is still lack of direct evidence in vivo.

Magnetic resonance imaging (MRI) has been considered to be the best research method of neuroscience in vivo[9, 10]. Using the sequences of T2 or T2*, brain iron have been detected in several neuro-diseases, however, these results were limited by significant technical deficiencies - non-quantitative measurement, in which phase signal was easily affected by the formation of the magnetic field distribution because of the nonlocal nature of the magnetic field distribution[11]. Quantitative susceptibility mapping (QSM) is an independent of field strength and object shape imaging that has been considered to be the optimum quantitative detection for brain iron[12, 13]. The successful application of this imaging technology in diseases (Huntington’s disease, Parkinson's disease, et al.) makes it possible to study the brain iron of patients with depression[14, 15].

Here, using QSM measure and voxel-based analyses, the objective of this study was to systematically investigate the changes of brain iron deposition in the whole brain and regions of interest (ROIs) of depressed patients, and to assess the relationships between susceptibility and depression-related conditions.

Subjects And Methods

Subjects

Basing on the results from the Chinese version of the Modified Structured Clinical Interview for DSM-IV, twenty-one depression patients were recruited from the Department of Neurology and Psychiatry. Inclusion criteria for enrollment included no previous history of neurological diseases, tumors, chronic diseases or head injuries. All subjects were scanned by 3T MR at baseline before treatment and follow-up after treatment (depressive symptoms disappeared, HRDS≤8), and received extended diagnostic examinations, including a review on clinical history, and a 24-item Hamilton Depression Rating Scale (HDRS) assessment. Additionally, according to the inclusion criteria, twenty control subjects (matched for age, sex, education, and handedness) were also recruited. Group demographic details are summarized in Table 1. All the examinations were performed with the understanding and written consent of each subject,

with approval from the ethics committee of the Lianyungang first people's Hospital (LYG-20180438), and in compliance with national legislation and Declaration of Helsinki guidelines.

Table 1
Study demographic details

	Control (n=20)	Depression (n=21)	
Sex (male/female)	9/11	9/12	NS
Age (years)	37.7±7.3	39.4±4.2	NS
Handedness (Right/Left)	21/0	21/0	NS
Education (years)	9.4±3.5	9.7±2.1	NS
Family history	NA	NA	
Outpatient/Inpatient	NA	0/21	
Unipolar/Bipolar	NA	21/0	
First-episode/ Relapse	NA	0/21	
HRDS (scores)	NA	27.2±5.3	
Relapse frequency (times)	NA	3.3±0.8	
Mean duration of single episode (weeks)	NA	8.4±1.1	
Total course of disease onset (weeks)	NA	24.4±2.6	
Values are given mean ± SD; NA=not applicable; NS=not significant (P>0.05).			
Total course of disease onset = cumulative single episode.			

Image Acquisition

All images were acquired using a Siemens Magnetom Trio 3.0T scanner with a 16-channel head coil. T1-weighted 3D-MPRAGE anatomical images were also collected to independently resolve the underlying brain anatomy. The imaging parameters were as follows: TR = 14ms with TE = 4.92ms, slice thickness = 1mm, flip angle = 7°, bandwidth/pixel = 140 Hz/pixel, voxel resolution = 1 × 1 ×1 mm^3, FOV = 25cm, matrix size = 256 × 256 ×192, scan time = 3 min 20 seconds and parallel imaging factors = 2. T2-weighted images were also acquired with turbo spin-echo for visual inspection to exclude brain abnormalities. The imaging parameters were as follows: TR = 5400ms with TE = 110ms, slice thickness = 2mm, flip angle = 150°, bandwidth/pixel = 140 Hz/pixel, turbo factor = 18, voxel resolution = 1 × 1 × 2 mm^3, FOV = 25cm, matrix size = 256 × 256, scan time = 2 min 40 seconds, and parallel imaging factors = 2. Gradient-recalled echo (GRE) data were collected as complex MRI signals from each receiver channel.

The imaging parameters were as follows: repeat time (TR) = 28ms with echo time (TE) = 16ms, slice thickness = 2mm, flip angle = 7°, bandwidth/pixel = 120Hz/pixel, voxel resolution = 1 × 1× 2 mm^3, FOV = 25cm, matrix size = 256 × 256×80 and scan time = 5min and 10 seconds. To minimize motion and increase inter-subject reproducibility in positioning, a thin pillow was placed on the base of the coil surrounding the sides and back of the head.

Data preprocessing

The magnitude images were projected with the BET algorithm (threshold setting 0.2) in the FMRIB Software Library (FSL) v5.0.9 (http://fsl.fmrib.ox.ac.uk/fsl/fslwiki/) to generate brain masks[16]. Phase images were unwrapped with the Laplacian approach[17]. Applying the method of SHARP filtering, the background field was removed using a kernel size with a maximum radius of 6 mm and a singular value decomposition threshold of 0.05[11]. Finally, an iterative algorithm was used to generate QSM images[18]. As previous study suggested that reference normalization is only of a small adjustment[19], susceptibility was not adjusted with a reference region in this study. The original susceptibility maps were derived from the following equation (for a left-handed system)[20]:

$$\Delta\chi = FT^{-1}\left[FT\left(-P_{cor} / (\gamma B_0 TE)\right) / \left(\frac{1}{3} - \frac{k_z^2}{k_x^2 + k_y^2 + k_z^2}\right)\right]$$

wherein, P_{cor} is the phase distribution of the unwrapped and background-field-corrected phase map; γ is the gyromagnetic ratio for hydrogen protons; B_0 is the main magnetic field strength; TE is the echo time; and k_x, k_y, k_z are coordinates in k-space.

Spatial standardization

To align pixels to the same anatomical position in the brains of different subjects, the following post-processing steps were performed using a Statistical Parametric Mapping Version 8 (SPM8) program (http://www.fil.ion.ucl.ac.uk/spm), which was run on matrix laboratory (MATLAB) 2013a (https://www.mathworks.com/products/matlab.html): The individual high-resolution MPRAGE -T1WIs were initially normalized to Montreal Neurological Institute (MNI), and co-registered to the QSM image after motion correction using a linear transformation. Then, the co-registered QSM images were normalized to MNI space using the normalized parameters of the MPRAGE-T1WIs. Applying the smoothing-compensation strategy proposed by a previously study[21], 3D Gaussian kernel (3 mm) was performed for correcting co-registration errors and other imperfections.

ROIs extraction

ROIs were extracted bilaterally in FSL according to the BN_Atlas_274_noCb_uint16 template (https://scalablebrainatlas.incf.org/human/BNA)[22]. In order to reduce the marginal effects caused by standardized defects and registration errors, ROIs were eroded in 3D by convolution with a 1-mm-radius

spherical kernel. Mask overlays were checked to ensure that all masks excluded spurious voxels. The iron concentration in postmortem samples as reported by Hallgren and Sourander was used to validate whether QSM data provided a reliable quantitative measure of iron[23].

Statistical methods

Whole-brain (depression versus control) permutation analysis was conducted with the Statistical nonParametric Mapping toolbox (SnPM) in SPM8. Significant clusters were determined with 20000 data permutations. A significance level of P=0.005 was applied with correction for multiple comparisons using the family-wise error (FWE) (P<0.05) method and clusters with at least 10 contiguous voxels. As a large number of previous studies have confirmed the positive effects of demographics (age, sex, medication, and so on) on iron content in the brain, these covariates were adjusted in group comparison[24]. After analysis, the study results were warped to MNI space and viewed in XJVIEW software (http://www.alivelearn.net/xjview).

Wilcoxon rank-sum tests were used to show interhemispheric differences. Then, averaged susceptibility of ROIs was used for comparison on tissue iron data, and averaged median susceptibility of ROIs across hemispheres were computed to improve measurement stability. Moreover, depression-versus-control Wilcoxon rank-sum statistics were computed ($P_{Bonferroni}$<0.05). The change of susceptibility before and after treatment in the depression was detected by paired t test. In addition, Pearson correlation test (median ROI susceptibility with symptom severity-HRDS, relapse frequency, mean duration of single episode, and total course of disease onset) was also computed, and linear least-square fits were calculated for regions where the Pearson correlation test returned a significant result. All tests were performed as two-tailed test.

Results

Individual comparison

Definite iron deposition in the brain were found in the basal ganglia and other deep-brain nuclei (the globus pallidus had a highest susceptibility), which were not so remarkable in the cortex. Moreover, the venous system and some small scattered signal inhomogeneities were found in maps. In addition, comparing with the controls, patients with depression showed significantly increased susceptibilities in the bilateral putamen and thalamus (Figure 1).

Whole-brain QSM study

The whole-brain group results revealed that iron deposition under depression is spatially selective (Figure 2). Besides, the whole-brain QSM results revealed widespread absolute susceptibility increases in patients with depression, which involved both the cerebellar and cerebral structures (FWE corrected P<0.05). Largely bilateral abnormalities were found in the frontal lobes, temporal lobe structures, occipital lobes hippocampal regions, putamen, thalamus, cingulum, and cerebellum of the patient group.

ROIs extraction and validation

The average susceptibility of ROIs from the control group in this study was compared with the iron concentration in postmortem samples as reported by a previous study[23]. Although there were significant differences between the two groups that might be attributable to some objective reasons (the former was dominated by ferritin macromolecules, myelin, blood, calcium and trace elements; the latter was dominated by non-haemin iron), a linear regression was then applied to find the correlation between susceptibility values of controls in the present study and iron content in postmortem samples from Hallgren and Sourander[23], and a significant correlation (r=0.783, P<0.001) was found in the frontal lobe, temporal lobe, occipital lobe, cerebellum, putamen, and thalamus (Supplementary Material 1).

Regional QSM study

Regional QSM study showed that left/right measurements were comparable across controls and patients with depression in both the deep gray matter (DGM) structures and cortex (all P>0.140). Compared with the control group, the depression group showed significantly increased regional susceptibility in the frontal lobe (Z= 3.6, P<0.001), temporal lobe (Z= 4.2, P<0.001), occipital lobe (Z= 4.3, P<0.001), hippocampus (Z= 3.0, P=0.007), putamen (Z= 3.4, P<0.001), thalamus (Z= 3.3, P<0.001), and cingulum (Z= 2.3, P=0.01), as well as in the cerebellum (Z= 2.8, P=0.004) (Supplementary Material 2).

Although HRDS showed significant differences before and after treatment (t=16.295, P=0.000), there was no susceptibility change was found in the involved brain regions (Supplementary Material 3), and no significant correlation between HDRS and susceptibility was found (all P>0.05). Subsequent results revealed a nearly statistically significant association between the relapse frequency and the susceptibility in the putamen, thalamus, and hippocampus (Figure 3), and similar results were also found in the analysis of mean duration of single episode (Figure 4). Further studies showed that susceptibility across the putamen (ρ^2 = 0.27, P<0.001), thalamus (ρ^2 = 0.21, P<0.001), and hippocampus (ρ^2 = 0.19, P<0.001) were strongly correlated with the total course of disease onset (Figure 5).

Discussion

This study was the first to report the relationships between brain iron deposition and multiple factors associated with depression (treatment, symptom severity-HRDS, relapse frequency, mean duration of single episode, and total course of disease onset). Our study discovered widespread increased susceptibility across the basal ganglia and cortex in depression, which could not be reversed by treatment. More important was the finding that susceptibility across the putamen, hippocampus, and thalamus were strongly correlated with the total course of disease onset, but not the severity of depressive status-HRDS. It is suggested that brain iron deposition may be a cumulative marker of brain damage in depression, but not an immediate indicator of symptoms.

Before the QSM method was successful developed[25, 26], there were two types of methods to detect iron in the brain, i.e., qualitative MRI methods (T2[27], T2*[28], R2*[29], SWI (susceptibility weighted imaging)

[30]), and semi-quantitative MRI methods (magnetic field correlation (MFC) imaging[31], phase imaging[32]). However, all the above-mentioned methods are essentially based on the characteristics of the magnetic field, which may cause blooming artifacts[33, 34], so the traditional MRI quantification methods do not provide an absolute quantification and are under the effect of non-local influences[35]. Compared to the traditional techniques, QSM is believed to be able to give a more accurate and specific measurement on tissue magnetic susceptibility[36, 37]. This susceptibility can be calculated using a map of the resonance frequency in each voxel, which traditionally utilizes the MR phase signal from GRE imaging and has been shown to correlate well with tissue iron concentration in most gray matter regions in the brain[38].

As iron deposition in the brain is spatially selective (significant brain iron deposition was found in the basal ganglia and other deep-brain nuclei), these ROIs are usually subjectively chosen, artificially outlined, extracted, and analyzed directly in most previous MRI researches. In fact, there are two major deficiencies with this strategy. First, it usually ignores the changes in the most important structure of the brain (the cortex). Abnormal deposition of iron in the cerebral cortex has been proved *in vitro* by other established methods, such as histochemical analysis, staining or transcranial sonography. Second, the extraction of artificially outlined ROIs is subject to two definite limitations: i) results are generally prone to inaccuracies in ROI definition due to the intricate anatomical substructures and weak contrast of anatomical boundaries on QSM; and ii) the poor consistency of repeated measurements depending on subjective outlining might cause a group-dependent study bias. In need of special is that, although ROIs extracted according to the MNI-template in FSL could overcome the above deficiencies, there was still limitation of the method adopted in this study that the registration might be not perfect because of lost or mixed image information.

In our study, consistent results from both a whole-brain and regional QSM study showed that brain regions with abnormal susceptibility in patients with depression included the frontal lobes, temporal lobes, occipital lobes, hippocampal regions, putamen, thalamus, cingulum, and cerebellum. We found it interesting that increased brain iron deposition occurred not only in two iron-rich areas (not all iron-rich brain areas were involved), but also in areas with minimal iron content (cortex, hippocampus and cerebellum). This phenomenon was also reported in previous QSM whole-brain studies of iron deposition in PD and MS patients[19, 24]. Although its intrinsic mechanism remains unclear, this distribution pattern of aberrant brain iron deposition is enough to draw our attention and strongly suggest that studies on iron in the brain should not be focused merely on DGM. So far, direct evidence of the relations between iron deposition patterns in the brain and depression has been exhibited in this study. In fact, regions of aberrant brain iron deposition we reported here were consistent with those reported by structural and fMRI studies of depression[39, 40]. That is, in a state of stress or depression, brain iron deposition may be one of physiological and pathological changes, with synergistic effects on the structure and function of the sensitive brain regions.

In subsequent analysis, we found the susceptibility in the involved brain regions could not be reversed by treatment, and was not correlated with the severity of depressive status-HRDS. The results were slightly

different from the previous reports[41], which might be explained by two reasons: (i) different sample populations and (ii) different methods of brain iron deposition analysis. Our further results found that not only the susceptibility in the putamen, thalamus and hippocampus presented a nearly statistically significant association with the relapse frequency and mean duration of single episode, but also a strongly correlated with the total course of disease onset. In fact, the relapse frequency and mean duration of single episode were the two determinations of the total course of disease onset. We believed that these three factors should be all closely related to the brain iron deposition in the above brain regions, and “a nearly statistically significant” might be attributed to the limited sample size in this study. Besides, it was not surprising to find that these regions of brain iron deposition were associated with the depression-related conditions, as previous studies had revealed that the putamen (part of the striatum) is related to motor and cognitive functions[42], and its dysfunction is known to be associated with loss of dopaminergic neurons within the cortical-striatum-thalamocortical circuit[4]. The thalamus is thought to be involved in the pathophysiology of depressive disorders and is currently drawing sustaining attention[43], and a recent research has reported that abnormal thalamocortical connectivity was found in depression[44]. Another brain region involved was the well-studied hippocampus, which has always been regarded as a targeted area in depression research because of its important role in emotion, cognition and memory. In general, brain iron deposition in the specific brain regions may be a cumulative marker of brain damage in depression, but not an immediate indicator of symptom.

We sincerely apologize for the shortcomings of the paper. 1) A limited sample size in this study could lead to statistical errors of type I and II. 2) We had not adopted a finer scale for the selection of cortical interest areas. 3) This study did not have sufficient follow-up to understand the further evolution of brain iron deposition in depression.

In conclusions, brain iron deposition is related to the total course of disease onset, but not the severity of depression, which suggest that brain iron deposition may be a sign of brain damage in multiple recurrent depression.

Abbreviations

QSM
Quantitative susceptibility mapping
ROI
Regions of interest
HRDS
Hamilton Depression Rating Scale
MRI
Magnetic resonance imaging
MNI
Montreal Neurological Institute
GRE

Gradient-recalled echo.

Declarations

Acknowledgements

Not applicable.

Authors' contributions

X.X.D, Y.H.X and L.L made a substantial contribution to the concept and design, analysis and interpretation of data; X.X.D and Y.H.X wrote the manuscript and provided figures; L.L, G.Q.F and Y.H.X revised the article critically for important intellectual content; X.F.Z, L.C and F.L. organized the study and supported the data analysis. All authors were critically involved in the theoretical discussion and performing of the experiments. All authors read and approved the final version of the manuscript.

Funding

This work was supported by Project of Jiangsu Health Committee (2017090), project of Zhenjiang social development (SH2019083, SH2019063, SH2018030).

Availability of data and materials

The datasets used and/or analyzed during the current study available from the corresponding author on reasonable request.

Ethics approval and consent to participate

This study was approved by the institutional review committees of the Lianyungang first people's Hospital (LYG-20180438), and written consents were obtained from all participants after they had received a complete and detailed description of the study.

Consent for publication

Written informed consent for the publication of clinical details and/or clinical images was obtained from all patients or their legal guardians.

Competing interests

The authors declare that they have no competing interests.

Author details

[1] Department of Radiology, Lianyungang first people's Hospital, Lianyungang, Jiangsu, China

[2] Department of Radiology, Affiliated hospital of jiangsu university, Zhenjiang, Jiangsu, China

References

1. Moylan S, Maes M, Wray N, Berk M. The neuroprogressive nature of major depressive disorder: pathways to disease evolution and resistance, and therapeutic implications. Molecular psychiatry. 2013;18 5:595–606; doi: 10.1038/mp.2012.33.
2. Li Y, Yan J, Zhu X, Zhu Y, Yao S, Xu Y, et al. Dilated Virchow-Robin spaces in the hippocampus impact behaviors and effects of anti-depressant treatment in model of depressed rats. Journal of affective disorders. 2017;219:17–24; doi: 10.1016/j.jad.2017.04.035.
3. Zhang N, Qin J, Yan J, Zhu Y, Xu Y, Zhu X, et al. Increased ASL-CBF in the right amygdala predicts the first onset of depression in healthy young first-degree relatives of patients with major depression. Journal of cerebral blood flow and metabolism: official journal of the International Society of Cerebral Blood Flow and Metabolism. 2020;40 1:54–66; doi: 10.1177/0271678x19861909.
4. Liu C, Liang M, Soong T. Nitric Oxide, Iron and Neurodegeneration. Frontiers in neuroscience. 2019;13:114; doi: 10.3389/fnins.2019.00114.
5. Muhoberac B, Vidal R. Iron, Ferritin, Hereditary Ferritinopathy, and Neurodegeneration. Frontiers in neuroscience. 2019;13:1195; doi: 10.3389/fnins.2019.01195.
6. Burhans M, Dailey C, Beard Z, Wiesinger J, Murray-Kolb L, Jones B, et al. Iron deficiency: differential effects on monoamine transporters. Nutritional neuroscience. 2005;8 1:31–8; doi: 10.1080/10284150500047070.
7. Bagnato F, Hametner S, Yao B, van Gelderen P, Merkle H, Cantor F, et al. Tracking iron in multiple sclerosis: a combined imaging and histopathological study at 7 Tesla. Brain: a journal of neurology. 2011;134:3602–15; doi: 10.1093/brain/awr278.
8. Dixon S, Stockwell B. The role of iron and reactive oxygen species in cell death. Nature chemical biology. 2014;10 1:9–17; doi: 10.1038/nchembio.1416.
9. Haacke E, Cheng N, House M, Liu Q, Neelavalli J, Ogg R, et al. Imaging iron stores in the brain using magnetic resonance imaging. Magnetic resonance imaging. 2005;23 1:1–25; doi: 10.1016/j.mri.2004.10.001.
10. Tambasco N, Paolini Paoletti F, Chiappiniello A, Lisetti V, Nigro P, Eusebi P, et al. T2*-weighted MRI values correlate with motor and cognitive dysfunction in Parkinson's disease. Neurobiology of aging. 2019;80:91–8; doi: 10.1016/j.neurobiolaging.2019.04.005.
11. Schweser F, Deistung A, Lehr B, Reichenbach J. Quantitative imaging of intrinsic magnetic tissue properties using MRI signal phase: an approach to in vivo brain iron metabolism? NeuroImage. 2011;54 4:2789–807; doi: 10.1016/j.neuroimage.2010.10.070.
12. Wang Y, Spincemaille P, Liu Z, Dimov A, Deh K, Li J, et al. Clinical quantitative susceptibility mapping (QSM): Biometal imaging and its emerging roles in patient care. Journal of magnetic resonance imaging: JMRI. 2017;46 4:951–71; doi: 10.1002/jmri.25693.

13. de Rochefort L, Liu T, Kressler B, Liu J, Spincemaille P, Lebon V, et al. Quantitative susceptibility map reconstruction from MR phase data using bayesian regularization: validation and application to brain imaging. Magnetic resonance in medicine. 2010;63 1:194–206; doi: 10.1002/mrm.22187.
14. Gong N, Dibb R, Bulk M, van der Weerd L, Liu C. Imaging beta amyloid aggregation and iron accumulation in Alzheimer's disease using quantitative susceptibility mapping MRI. NeuroImage. 2019;191:176–85; doi: 10.1016/j.neuroimage.2019.02.019.
15. Xiao B, He N, Wang Q, Cheng Z, Jiao Y, Haacke E, et al. Quantitative susceptibility mapping based hybrid feature extraction for diagnosis of Parkinson's disease. NeuroImage Clinical. 2019;24:102070; doi: 10.1016/j.nicl.2019.102070.
16. Smith S. Fast robust automated brain extraction. Human brain mapping. 2002;17 3:143–55; doi: 10.1002/hbm.10062.
17. Schofield M, Zhu Y. Fast phase unwrapping algorithm for interferometric applications. Optics letters. 2003;28 14:1194–6; doi: 10.1364/ol.28.001194.
18. Tang J, Liu S, Neelavalli J, Cheng Y, Buch S, Haacke E. Improving susceptibility mapping using a threshold-based K-space/image domain iterative reconstruction approach. Magnetic resonance in medicine. 2013;69 5:1396–407; doi: 10.1002/mrm.24384.
19. Acosta-Cabronero J, Cardenas-Blanco A, Betts M, Butryn M, Valdes-Herrera J, Galazky I, et al. The whole-brain pattern of magnetic susceptibility perturbations in Parkinson's disease. Brain: a journal of neurology. 2017;140 1:118–31; doi: 10.1093/brain/aww278.
20. Haacke E, Tang J, Neelavalli J, Cheng Y. Susceptibility mapping as a means to visualize veins and quantify oxygen saturation. Journal of magnetic resonance imaging: JMRI. 2010;32 3:663–76; doi: 10.1002/jmri.22276.
21. Betts M, Acosta-Cabronero J, Cardenas-Blanco A, Nestor P, Düzel E. High-resolution characterisation of the aging brain using simultaneous quantitative susceptibility mapping (QSM) and R2* measurements at 7T. NeuroImage. 2016;138:43–63; doi: 10.1016/j.neuroimage.2016.05.024.
22. Fan L, Li H, Zhuo J, Zhang Y, Wang J, Chen L, et al. The Human Brainnetome Atlas: A New Brain Atlas Based on Connectional Architecture. Cerebral cortex (New York, NY: 1991). 2016;26 8:3508-26; doi: 10.1093/cercor/bhw157.
23. HALLGREN B, SOURANDER P. The effect of age on the non-haemin iron in the human brain. Journal of neurochemistry. 1958;3 1:41–51; doi: 10.1111/j.1471-4159.1958.tb12607.x.
24. Acosta-Cabronero J, Betts M, Cardenas-Blanco A, Yang S, Nestor P. In Vivo MRI Mapping of Brain Iron Deposition across the Adult Lifespan. The Journal of neuroscience: the official journal of the Society for Neuroscience. 2016;36 2:364–74; doi: 10.1523/jneurosci.1907-15.2016.
25. Liu W, Ge T, Leng Y, Pan Z, Fan J, Yang W, et al. The Role of Neural Plasticity in Depression: From Hippocampus to Prefrontal Cortex. Neural plasticity. 2017;2017:6871089; doi: 10.1155/2017/6871089.
26. Stüber C, Pitt D, Wang Y. Iron in Multiple Sclerosis and Its Noninvasive Imaging with Quantitative Susceptibility Mapping. International journal of molecular sciences. 2016;17 1; doi:

10.3390/ijms17010100.

27. Vymazal J, Brooks R, Zak O, McRill C, Shen C, Di Chiro G. T1 and T2 of ferritin at different field strengths: effect on MRI. Magnetic resonance in medicine. 1992;27 2:368–74; doi: 10.1002/mrm.1910270218.
28. Chavhan G, Babyn P, Thomas B, Shroff M, Haacke E. Principles, techniques, and applications of T2*-based MR imaging and its special applications. Radiographics: a review publication of the Radiological Society of North America, Inc. 2009;29 5:1433–49; doi: 10.1148/rg.295095034.
29. Deistung A, Schäfer A, Schweser F, Biedermann U, Turner R, Reichenbach J. Toward in vivo histology: a comparison of quantitative susceptibility mapping (QSM) with magnitude-, phase-, and R2*-imaging at ultra-high magnetic field strength. NeuroImage. 2013;65:299–314; doi: 10.1016/j.neuroimage.2012.09.055.
30. Haacke E, Makki M, Ge Y, Maheshwari M, Sehgal V, Hu J, et al. Characterizing iron deposition in multiple sclerosis lesions using susceptibility weighted imaging. Journal of magnetic resonance imaging: JMRI. 2009;29 3:537–44; doi: 10.1002/jmri.21676.
31. Ropele S, de Graaf W, Khalil M, Wattjes M, Langkammer C, Rocca M, et al. MRI assessment of iron deposition in multiple sclerosis. Journal of magnetic resonance imaging: JMRI. 2011;34 1:13–21; doi: 10.1002/jmri.22590.
32. Ogg R, Langston J, Haacke E, Steen R, Taylor J. The correlation between phase shifts in gradient-echo MR images and regional brain iron concentration. Magnetic resonance imaging. 1999;17 8:1141–8; doi: 10.1016/s0730-725x(99)00017-x.
33. Jensen J, Chandra R, Ramani A, Lu H, Johnson G, Lee S, et al. Magnetic field correlation imaging. Magnetic resonance in medicine. 2006;55 6:1350–61; doi: 10.1002/mrm.20907.
34. Li J, Chang S, Liu T, Wang Q, Cui D, Chen X, et al. Reducing the object orientation dependence of susceptibility effects in gradient echo MRI through quantitative susceptibility mapping. Magnetic resonance in medicine. 2012;68 5:1563–9; doi: 10.1002/mrm.24135.
35. Yablonskiy D, Haacke E. Theory of NMR signal behavior in magnetically inhomogeneous tissues: the static dephasing regime. Magnetic resonance in medicine. 1994;32 6:749–63; doi: 10.1002/mrm.1910320610.
36. Lim I, Faria A, Li X, Hsu J, Airan R, Mori S, et al. Human brain atlas for automated region of interest selection in quantitative susceptibility mapping: application to determine iron content in deep gray matter structures. NeuroImage. 2013;82:449–69; doi: 10.1016/j.neuroimage.2013.05.127.
37. Schweser F, Sommer K, Deistung A, Reichenbach J. Quantitative susceptibility mapping for investigating subtle susceptibility variations in the human brain. NeuroImage. 2012;62 3:2083–100; doi: 10.1016/j.neuroimage.2012.05.067.
38. Schenck J. The role of magnetic susceptibility in magnetic resonance imaging: MRI magnetic compatibility of the first and second kinds. Medical physics. 1996;23 6:815–50; doi: 10.1118/1.597854.

39. Zhao K, Liu H, Yan R, Hua L, Chen Y, Shi J, et al. Altered patterns of association between cortical thickness and subcortical volume in patients with first episode major depressive disorder: A structural MRI study. Psychiatry research Neuroimaging. 2017;260:16–22; doi: 10.1016/j.pscychresns.2016.12.001.
40. Sacchet M, Camacho M, Livermore E, Thomas E, Gotlib I. Accelerated aging of the putamen in patients with major depressive disorder. Journal of psychiatry & neuroscience: JPN. 2017;42 3:164–71; doi: 10.1503/jpn.160010.
41. Yao S, Zhong Y, Xu Y, Qin J, Zhang N, Zhu X, et al. Quantitative Susceptibility Mapping Reveals an Association between Brain Iron Load and Depression Severity. Frontiers in human neuroscience. 2017;11:442; doi: 10.3389/fnhum.2017.00442.
42. Herrero M, Barcia C, Navarro J. Functional anatomy of thalamus and basal ganglia. Child's nervous system: ChNS : official journal of the International Society for Pediatric Neurosurgery. 2002;18 8:386–404; doi: 10.1007/s00381-002-0604-1.
43. Kong L, Chen K, Womer F, Jiang W, Luo X, Driesen N, et al. Sex differences of gray matter morphology in cortico-limbic-striatal neural system in major depressive disorder. Journal of psychiatric research. 2013;47 6:733–9; doi: 10.1016/j.jpsychires.2013.02.003.
44. Brown E, Clark D, Hassel S, MacQueen G, Ramasubbu R. Thalamocortical connectivity in major depressive disorder. Journal of affective disorders. 2017;217:125–31; doi: 10.1016/j.jad.2017.04.004.

Figures

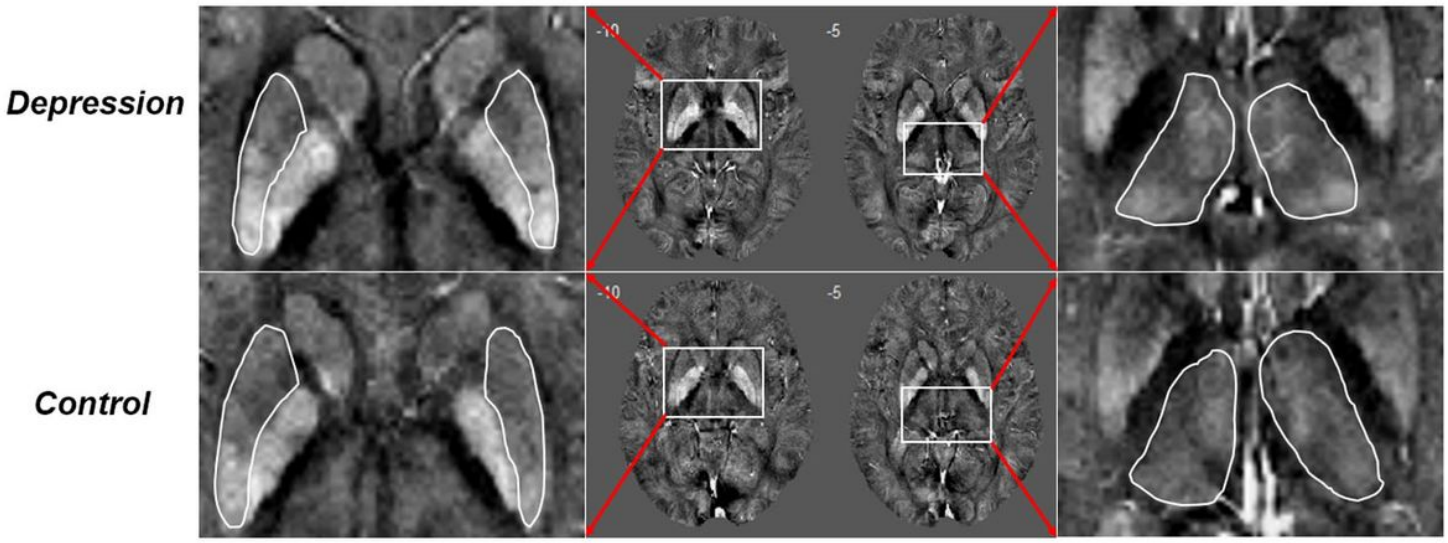

Figure 1

Patient with depression versus the control. Bright regions reflect the strong paramagnetism returned by metallic species such as tissue iron. Increased susceptibility in the bilateral putamen and thalamus could

be directly found.

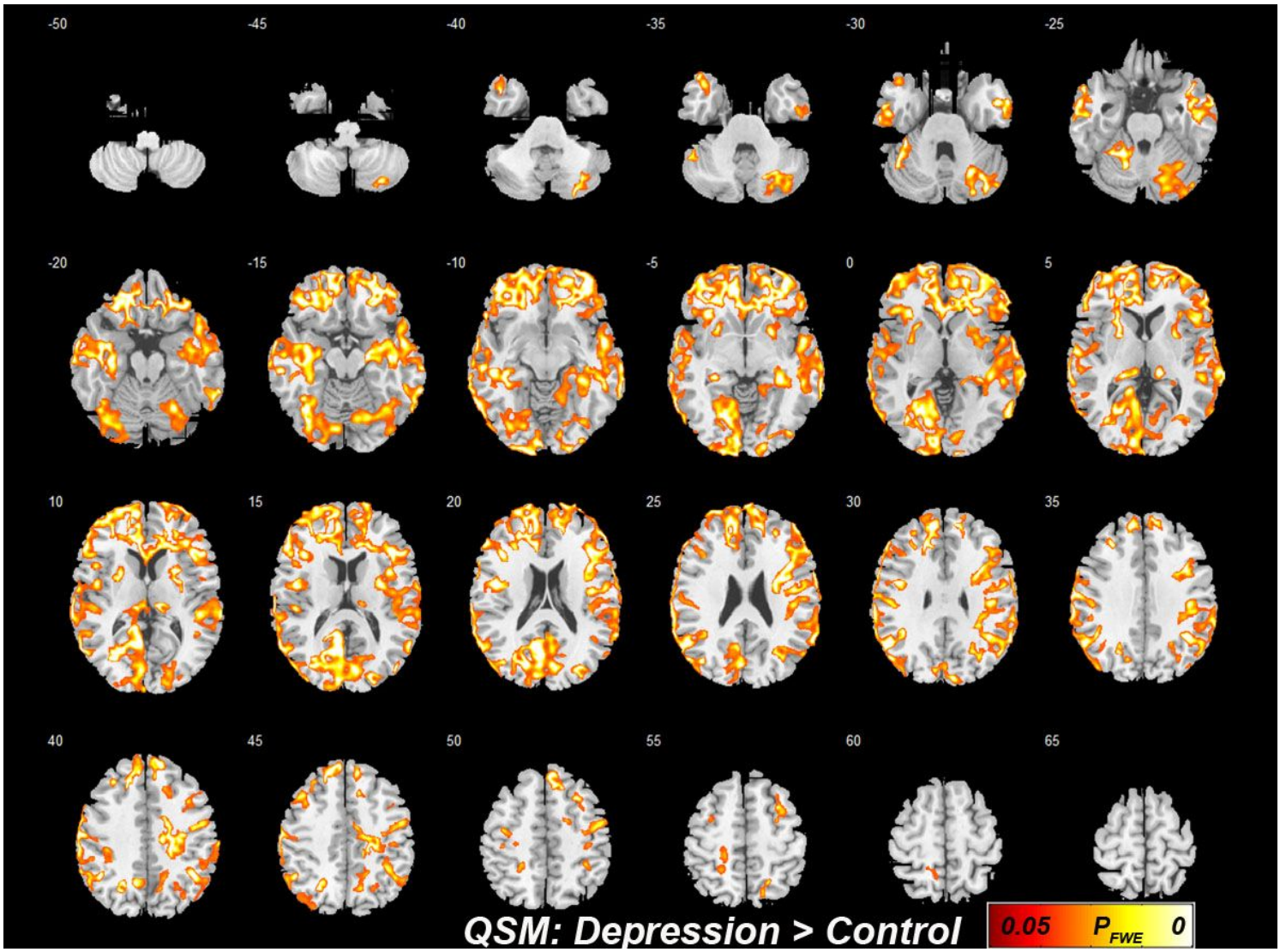

Figure 2

Results of the voxel-based analysis of corrected susceptibility between the control groups and patients with depression. The results were overlaid onto the MINI274 brain template and viewed in XJVIEW. Red/yellow clusters represent T values at PFWE<0.05.

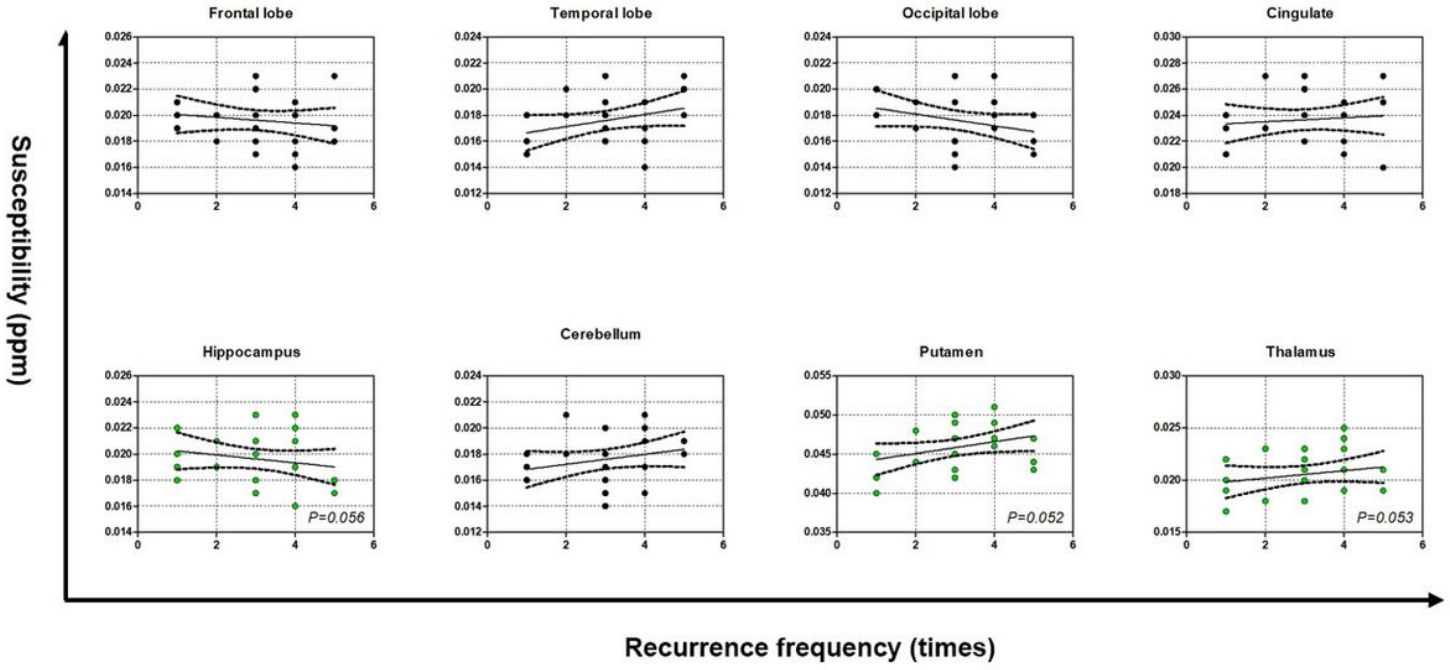

Figure 3

Median susceptibility for patients with depression plotted in relation to the relapse frequency. Dashed lines represent 95% confidence intervals.

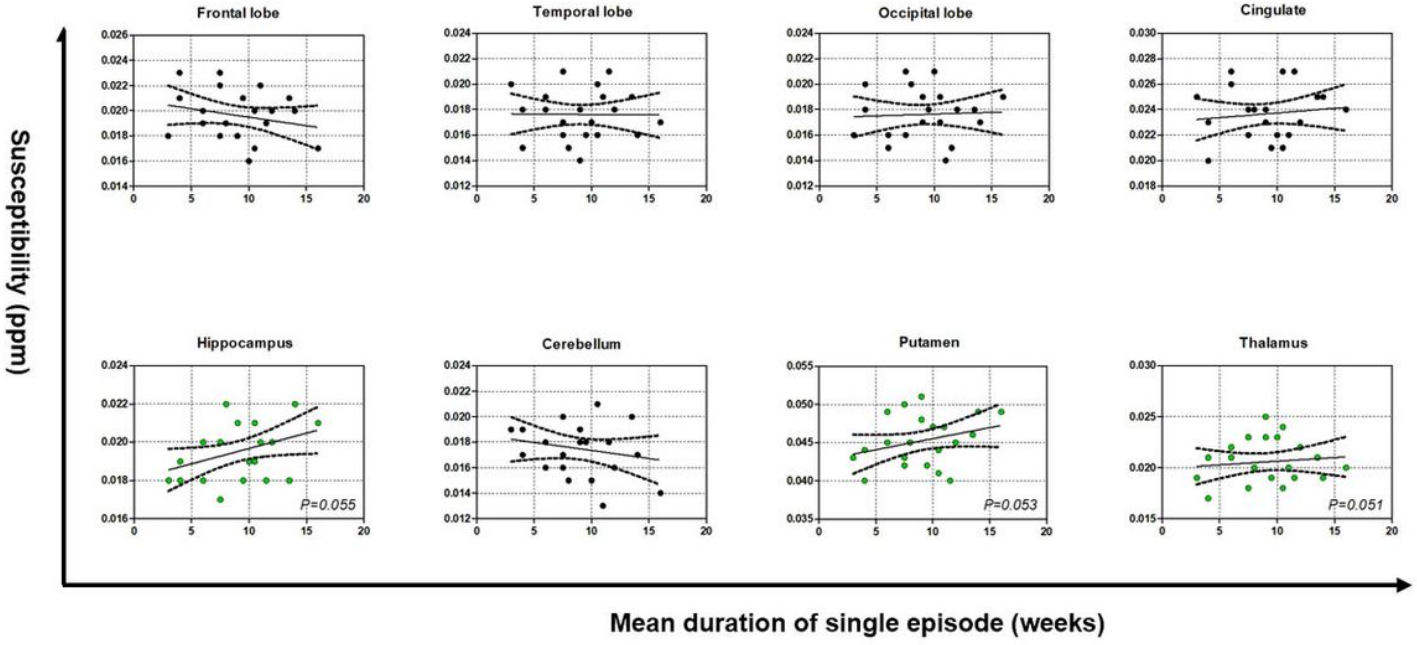

Figure 4

Median susceptibility for patients with depression plotted in relation to the mean duration of single episode. Dashed lines represent 95% confidence intervals.

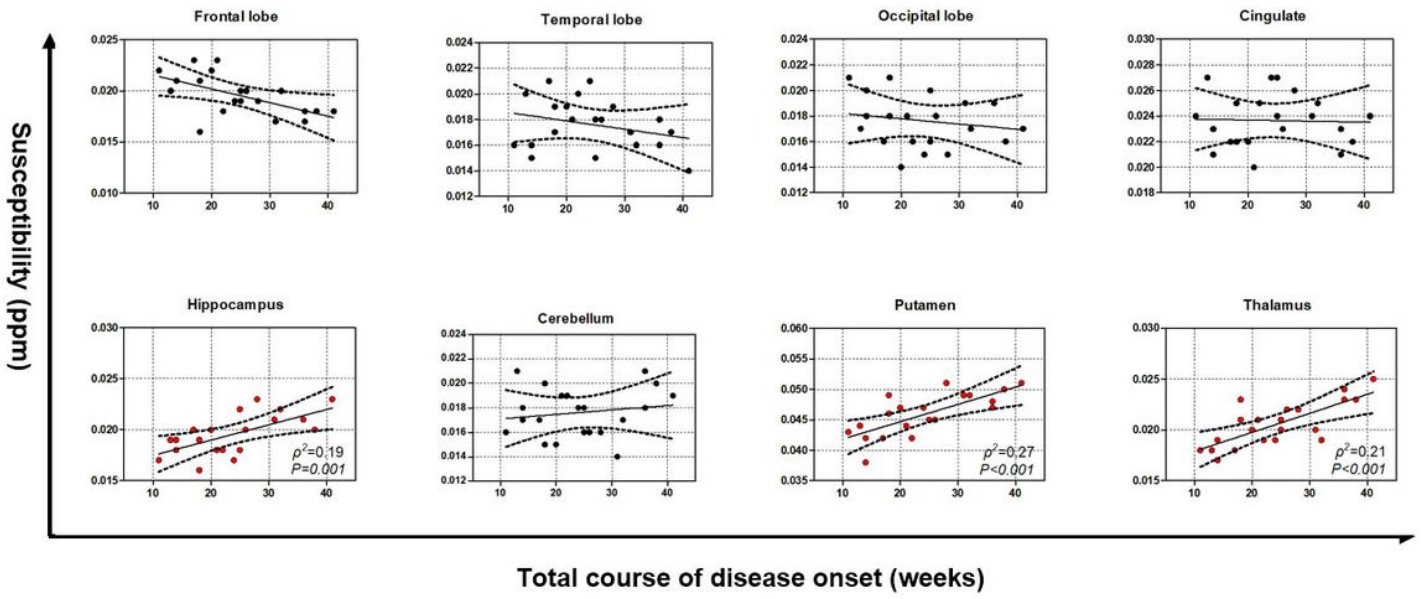

Figure 5

Median susceptibility for patients with depression plotted in relation to the total course of disease onset. Dashed lines represent 95% confidence intervals.

Supplementary Files

This is a list of supplementary files associated with this preprint. Click to download.

- SupplementaryMaterial.doc